Implications for the Formation of the Hollywood Basin from Gravity Interpretations of the Northern Los Angeles Basin, California

by Thomas G. Hildenbrand, Jeffrey G. Davidson, Daniel J. Ponti, and V.E. Langenheim

Open-File Report 2001-394

2001

This report is preliminary and has not been reviewed for conformity with U.S. Geological Survey editorial standards or with the North American Stratigraphic Code. Any use of trade, firm, or product names is for descriptive purposes only and does not imply endorsement by the U.S. Government.

TABLE OF CONTENTS

ILLUSTRATIONS

ABSTRACT

Gravity data provide insights on the complex tectonic history and structural development of the northern Los Angeles Basin region. The Hollywood basin appears to be a long (> 12 km), narrow (up to 2 km wide) trough lying between the Santa Monica Mountains and the Wilshire arch. In the deepest parts of the Hollywood basin, the modeled average thickness ranges from roughly 250 m if filled with only Quaternary sediments to approximately 600 m if Pliocene sediments are also present. Interpretations of conflicting drill hole data force us to consider both these scenarios. Because of the marked density contrast between the dense Santa Monica Mountains and the low-density sediments in the Los Angeles Basin, the gravity method is particularly useful in mapping the maximum displacement along the Santa Monica-Hollywood-Raymond fault zone. The gravity-defined Santa Monica–Hollywood fault zone deviates, in places, from the mapped active fault and fold scarps located with boreholes and trenching and by geomorphological mapping by Dolan and others (1997). Our models suggest that the Santa Monica–Hollywood fault zone dips northward approximately 63°. Three structural models are considered for the origin of the Hollywood basin: pull-apart basin, flexural basin, and a basin related to a back limb of a major fold. Although our preferred structural model involves flexure, the available geologic and geophysical data do not preclude contributions to the deepening of the basin from one or both of the other two models.

Of particular interest is that the distribution of red-tagged buildings and structures damaged by the Northridge earthquake has a strong spatial correlation with the axis of the Hollywood basin defined by the gravity data. Several explanations for this correlation are explored, but two preferred geologic factors for the amplification of ground motion besides local site effects are (1) focussing of energy by a fault along the axis of the Hollywood basin and (2) focussing effects related to differential refraction of seismic rays across the basin.

INTRODUCTION

A synthesis of gravity, geologic, and physical property data helps define geologic structures of the northern Los Angeles Basin region. The main goal of this data synthesis is to better characterize the upper 6 km of this seismogenic region. Although considerable information on this region exists in the literature (for example, Yerkes and others, 1965; Wright, 1991; Hummon, 1994), a detailed gravity study can provide new insights on the subsurface.

The Santa Monica-Hollywood-Raymond fault zone represents the northern boundary of the Los Angeles Basin. The Hollywood basin is a small sedimentary depression (< 1 km thick) that abuts the Santa Monica–Hollywood fault zone on the south (Fig. 1). The existence of the Hollywood basin was first proposed from water wells in a hydrologic study of the Los Angeles Basin (Eckis, 1934). Hummon and others (1994) provide the most recent description of the Hollywood basin in the form of structural contours on the base of Quaternary, based on limited drill hole data. Thus the geometry of the Hollywood basin is poorly known. Moreover, from their interpretive cross sections of the Hollywood basin, a thick layer of Quaternary sediment may lie directly above Miocene sediments, or thinner Quaternary layer above Pliocene siltstone and

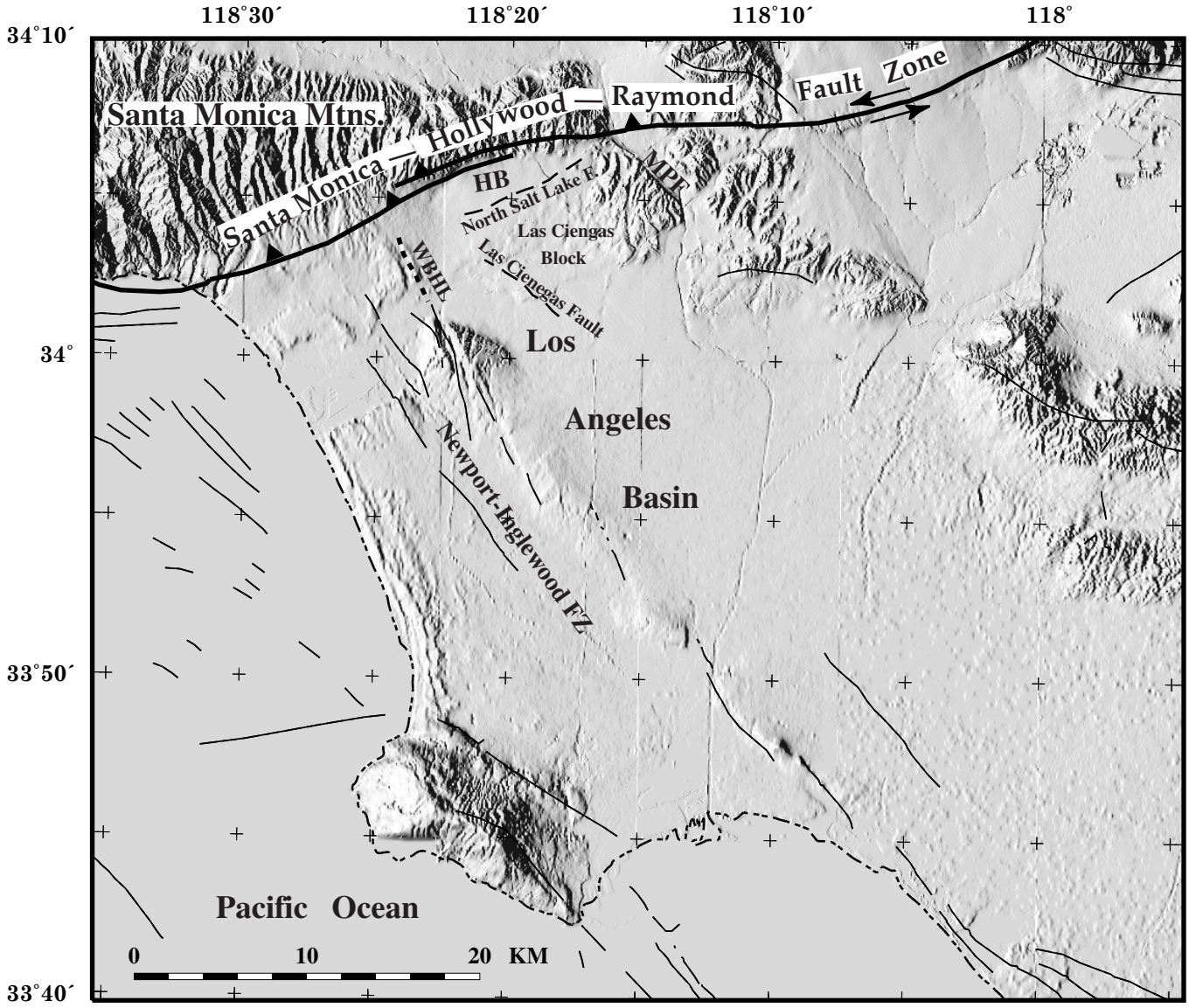

Figure 1. Shaded topographic map of the Los Angeles Basin region. WBHL and HB highlights, respectively, the West Beverly Hills lineament (Tsutsumi and others, 2001) and the Hollywood basin lying south of the Santa Monica-Hollywood fault zone. Black lines are faults from Jennings (1994).

shale may comprise the basin fill. Our synthesis of gravity, geologic, and physical property data is an attempt to provide a better understanding of the geometry and physical properties related to both the Hollywood basin and Santa Monica–Hollywood fault zone.

The gravity method is a cost-effective approach to examine hidden 3D structures in an urban environment, because cultural noise such as buildings has little or no effect on a gravity measurement. To effectively define the geometry of this local basin, more than 300 new gravity stations were collected to fill in the existing regional database. The gravity data are filtered here to enhance particular anomaly characteristics such as wavelength and trend. Several gravity inversion models are generated to define the geometry of local structures such as the Hollywood basin and Santa Monica–Hollywood fault zone. The interpretive results are then used to provide new insights into the geologic framework of the northern Los Angeles area and to explore the origin of the Hollywood basin and its possible effect on the seismic hazard in this heavily populated area.

GEOLOGIC HISTORY

The major structural elements of the study area are the Los Angeles Basin and Santa Monica Mountains. The Cenozoic Los Angeles Basin, containing more than 10 km of Neogene to Quaternary sediment (Yerkes and others, 1965), formed within the dynamic San Andreas transform zone. The Santa Monica Mountains bound the Los Angeles Basin on the north and are part of the central Transverse Range Province (Durrell, 1954; Dibblee, 1982). The Los Angeles Basin is linked to major right-lateral displacement on the San Andreas zone and clockwise rotation (as much as 100°) of crustal blocks within the Transverse Ranges (for example, Luyendyk and others, 1980). In Miocene time, a transextensional stress regime related to the clockwise-rotating blocks led to major left-lateral offsets on block-bounding faults. Some have suggested that during this stress regime (about 16 - 17 Ma until the end of Miocene), movement on the Santa Monica-Hollywood-Raymond fault zone was largely left-lateral with a total estimated offset ranging from 26 to 90 km (Wright, 1991). More current data, however, indicate that the offset is about 13-14 km occurring after 7 Ma (McCulloh and others, 2001).

The present form and structural relief of the Los Angeles Basin were established chiefly during a phase of accelerated subsidence and deposition that was initiated in latest Miocene and continued without significant interruption into the early Pleistocene (Lamar, 1961). Vertical movement associated with the opening of the Los Angeles Basin resulted in numerous folds and faults in the footwall of the Santa Monica-Hollywood fault zone. A pervasive east-northeast structural trend evolved (Fig. 1). For example, Wright (1991) suggested that "the North Salt Lake fault may have formed at this time by extension behind the uplifted Las Cienegas basement block that was sagging laterally into the deeply subsided basin to the southwest." The North Salt Lake fault, a steeply-dipping normal fault, may form the southern margin of the Hollywood basin (Wright, 1991). The Santa Monica Mountains experienced significant uplift at about 7 Ma during middle Puente time (Fig. 2; Wright, 1991).

Since mid-Pliocene time, additional major uplift of the Santa Monica Mountains occurred during a compressional stress regime (Wright, 1991). Dolan

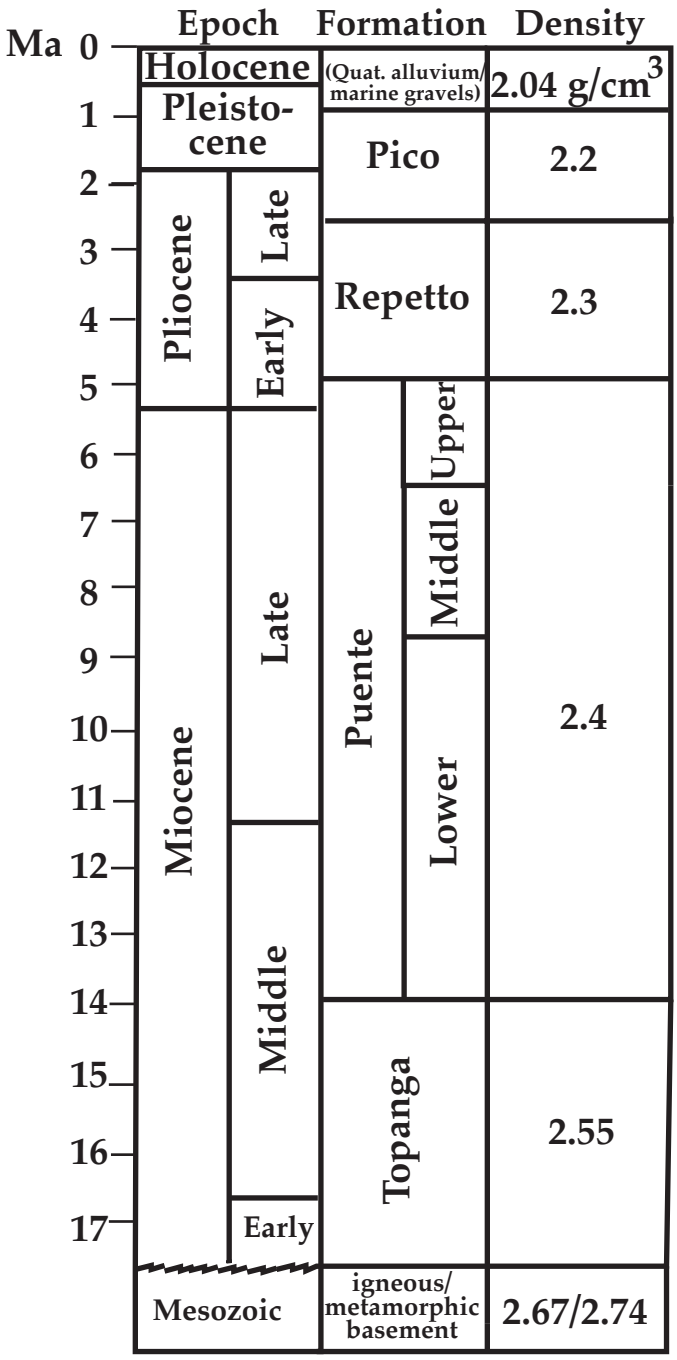

Figure 2. Stratigraphy of the northern Los Angeles region. Modified from Hummon (1994).

and others (1997) pointed out that a southward dip of Pleistocene marine platforms suggests Quaternary uplift of the Santa Monica Mountains (near longitude 118° 21′). The major strands of the Santa Monica-Hollywood-Raymond fault zone are the range front thrust faults defining the northern boundary of the Los Angeles Basin. At the present time, tectonism in the northern and northeastern parts of the Los Angeles Basin reflects the interaction between northwestward motion of the Pacific plate and north-south compressive shortening of the Transverse Ranges (Campbell and Yerkes, 1976). Based on geomorphologic mapping, Dolan and others (2000) found evidence for at least one surface-rupturing earthquake during the past ~ 22,000 years on a strand of the oblique, reverse-left-lateral Hollywood Fault, which dips steeply (≥ 75°) to the north.

Pre-Cenozoic basement in the Santa Monica Mountains and underlying the northern Los Angeles Basin may be part of the same late-Mesozoic calc-alkaline island-arc system (Sorensen, 1985). Basement drill holes in the Los Angeles Basin encounter primarily slate and schist (Wright, 1991). In the Santa Monica Mountains, basement consists of regionally metamorphosed Santa Monica slate. North of the Hollywood fault, the slate is intruded by Cretaceous plutons of granite, granodiorite, and quartz diorite (Fig. 3).

Prior to development of the Los Angeles Basin, sandstone, conglomerate, and volcanic rock (basalt flows) of the Topanga formation were deposited on pre-Cenozoic basement during rifting and the rotation of the Transverse Ranges in the early to middle Miocene (Wright, 1991). Younger volcanic rocks, generally diabase, are related to major volcanism in the very earliest Middle Miocene, during the rifting, rafting, and rotation of this region (Wright, 1991). During the late middle and late Miocene time, subsidence led to the deposition of a thick section of sedimentary rocks of the Puente Formation, which includes deep sea fans. After about 7 Ma, deposition within the Los Angeles Basin led to the Pliocene to early Pleistocene Repetto and Pico Formations, middle Pleistocene marine gravel and sand, and late Pleistocene and Holocene alluvium (Yerkes and others, 1965; Blake, 1991; Hummon and others, 1994). Quaternary sedimentary deposits are largely unconsolidated and uncemented (Yerkes and others, 1965).

GRAVITY DATA

New gravity measurements were made primarily along 12 profiles at a spacing of 200 m or better (squares, Fig. 4). In order to optimize the accuracy of the observed gravity readings, each station was sampled multiple times using two LaCoste and Romberg meters (Davidson and others, 1999). The accuracy of these new measurements should be in the range of 0.01 to 0.1 mGal.

These 315 new USGS gravity stations were combined with existing data from the Department of Defense (DOD) database to produce the coverage shown in Figure 4. All values were tied to the gravity datum based on the International Gravity Standardization Net of 1971 (Morelli, 1974) and reduced to complete Bouguer anomaly values using a reduction density of 2.67 g/cc and the 1967 formula for the theoretical gravity (Cordell and others, 1982). These data were then processed through an isostatic reduction program (Jachens and Roberts, 1981) in order to suppress the effects of deep density distributions that buoyantly support the topography. The resulting residual isostatic anomaly values for each

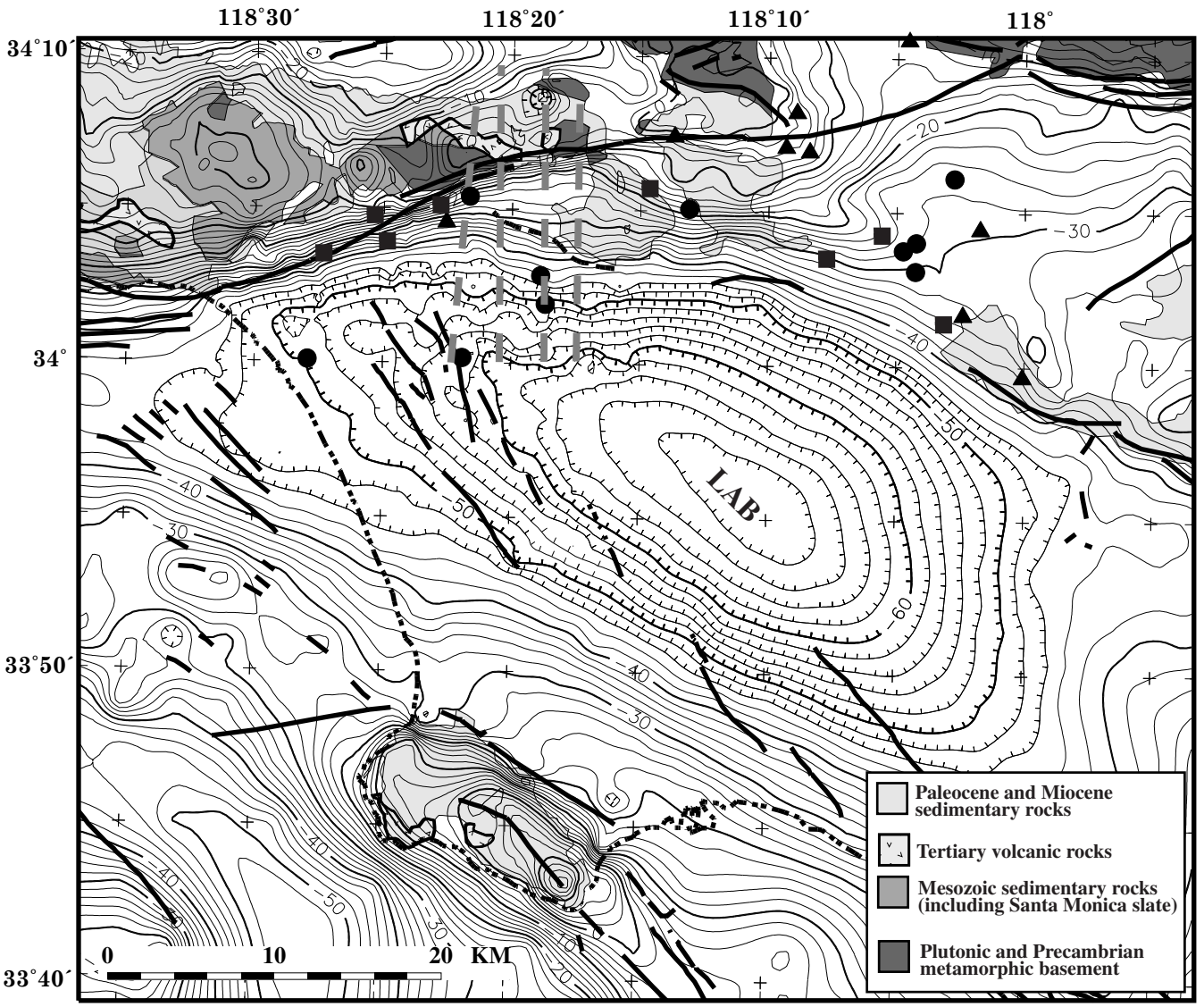

Figure 3. Isostatic residual gravity anomaly map and simplified geology of the Los Angeles Basin (LAB) region. The results of the inversion of gravity data along the profiles shown as dashed gray lines are found in Figure 7. Symbols represent wells encountering schist (circles), Santa Monica slate (squares), and granite (triangles) (taken from a USGS well data base).

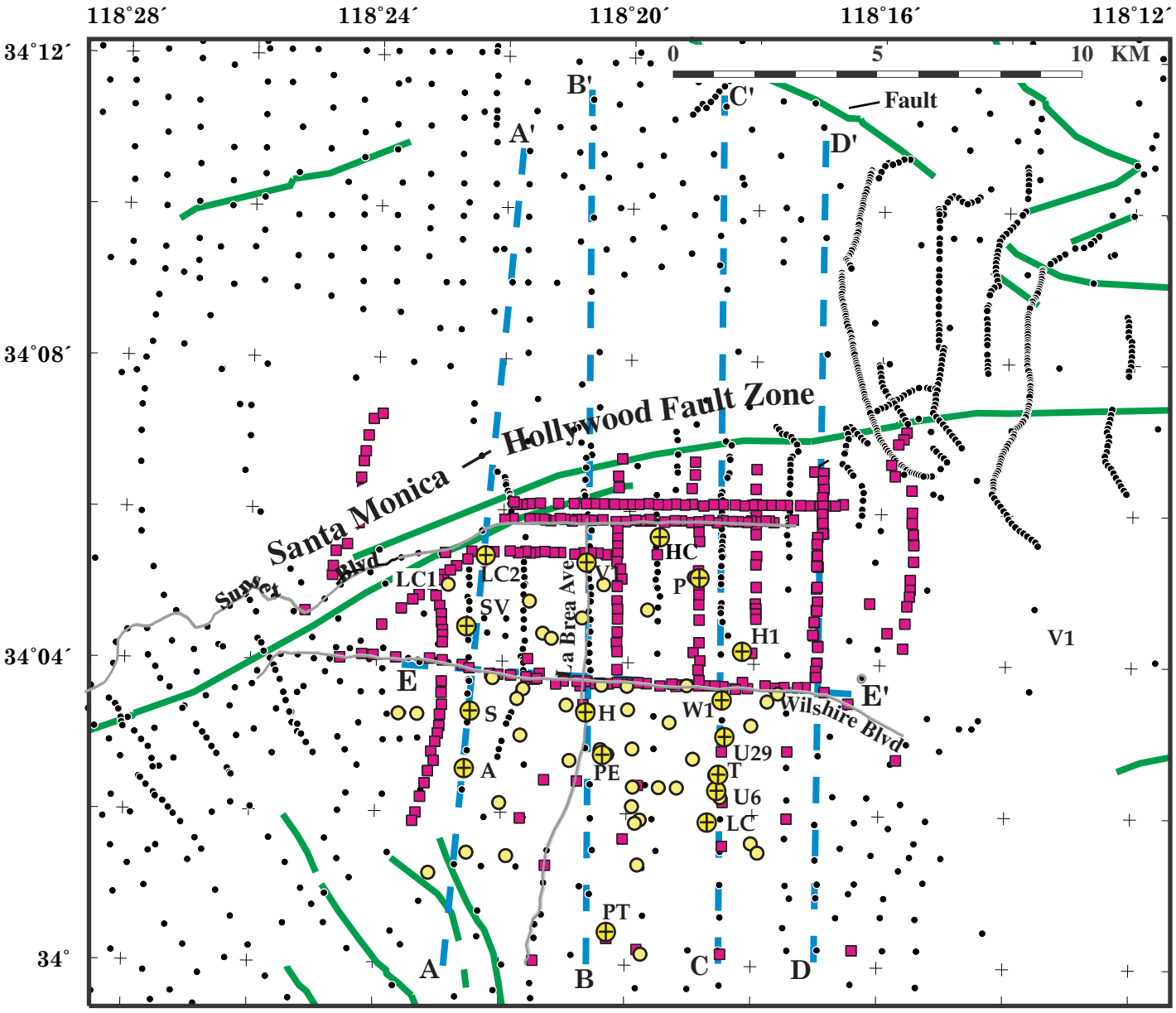

Figure 4. Gravity stations used to generate the anomaly map shown in Figure 3. Black dots and magenta squares are existing and new gravity stations, respectively. Cyan dashed lines are modeled profiles AA' through DD' shown in Figures 7 and 8. Yellow circles are locations of wells used by Hummon (1994) to generate geologic cross sections. Larger yellow circles with +'s denote deep wells used to constrain the models in Figure 7 and include: Profile AA'— Adamson CH1 (A), Saturn CH1 (S), San Vicente (SV), and Laurel CH2 (LC2); Profile BB'—Pacific Telephone CH1 (PT), Las Cienegas PE (PE), Highland (H), Yanveh CH1 (Y), and Vista CH1 (V1); Profile CC'—Las Cienegas Murphy (LC), Union CH6 (U6), Texam U-19 (T), Union CH29 (U29), Wilton CH1 (W1), Hobart CH1 (H1), Paramount U-14 (P), and Hollywood CH1 (HC). LC1 locates drill hole Laurel CH1, which is also shown in Figure 6. Green lines depict faults (Jennings, 1994). Gray lines show a few major streets.

station were gridded at a spacing of 0.5 km using minimum curvature and the computer algorithm of Webring (1982).

INTERPRETIVE TECHNIQUES

The gravity data were processed by computer to enhance density boundaries and shallow mass sources and to invert the gravity to define source geometries, depths, and densities, in order to provide geospatial and physical constraints for the Santa Monica–Hollywood fault zone, Hollywood basin, and other related structures.

Density Boundaries

An automatic gradient analysis method (Blakely and Simpson, 1986) was used to emphasize density boundaries because maxima in the horizontal gradient of the gravity field occur near steep boundaries separating contrasting densities. These gradient maxima are shown as small white dots on Figure 5a. Alignments of these dots are interpreted to mark steeply–dipping boundaries across which density differs (highlighted with black lines). The density boundary in the vicinity of the Santa Monica-Hollywood fault zone defines the juxtaposition of dense pre-Cenozoic rocks in the Santa Monica Mountains and low-density sedimentary rocks in the Los Angeles basin (in other words, the maximum displacement along the fault zone). Although generally consistent with surface mapping, this boundary does deviate from the mapped locations of faults (white lines, Fig. 5; Jennings, 1994) and major fault or fold scarps (magenta lines; Dolan and others, 1997).

Shallow Sources

Gravity anomaly maps exhibit the combined effects of geologic bodies of distinctive densities, which may have varying shapes, dimensions, and burial depths. Thus the gravity field is caused by the superposition of signals from many different bodies at differing depths. In order to accentuate the shallow-source anomalies, we applied a continuation filtering process designed to obtain a separation of long wavelength anomalies from short wavelength anomalies. The gravity data were upward continued 100 m (the grid interval) to smooth the gravity field; then the upward continued grid was subtracted from the original residual isostatic anomaly grid, leaving a 100 m upward continued residual grid. The resulting residual anomaly map shown in Figure 5b enhances the effects of shallow sources. Many gravity features in the unfiltered data are now apparent in the residual isostatic map, such as the narrow, linear low over the Hollywood basin, that extends at least 12 km from longitude 118°23′ to 118° 16′. A subtle gradient expresses the North Salt Lake fault. The gravity high south of the North Salt Lake fault defines the Wilshire arch of Hummon (1994) or the northern shelf monocline of Wright (1991). The pronounced east-northeast trending gradient north of the Hollywood basin clearly defines the range front thrusts related to the Santa Monica-Hollywood fault zone.

Inversion Models

The principal goal of a gravity study is to detect and quantify changes in density at depth and to make reasonable geologic inferences based on these interpreted geometries and properties. Translation of the observed gravity anomalies into a meaningful geologic picture of the subsurface requires an inverse modeling method. We used a 2 1/2 dimensional modeling program

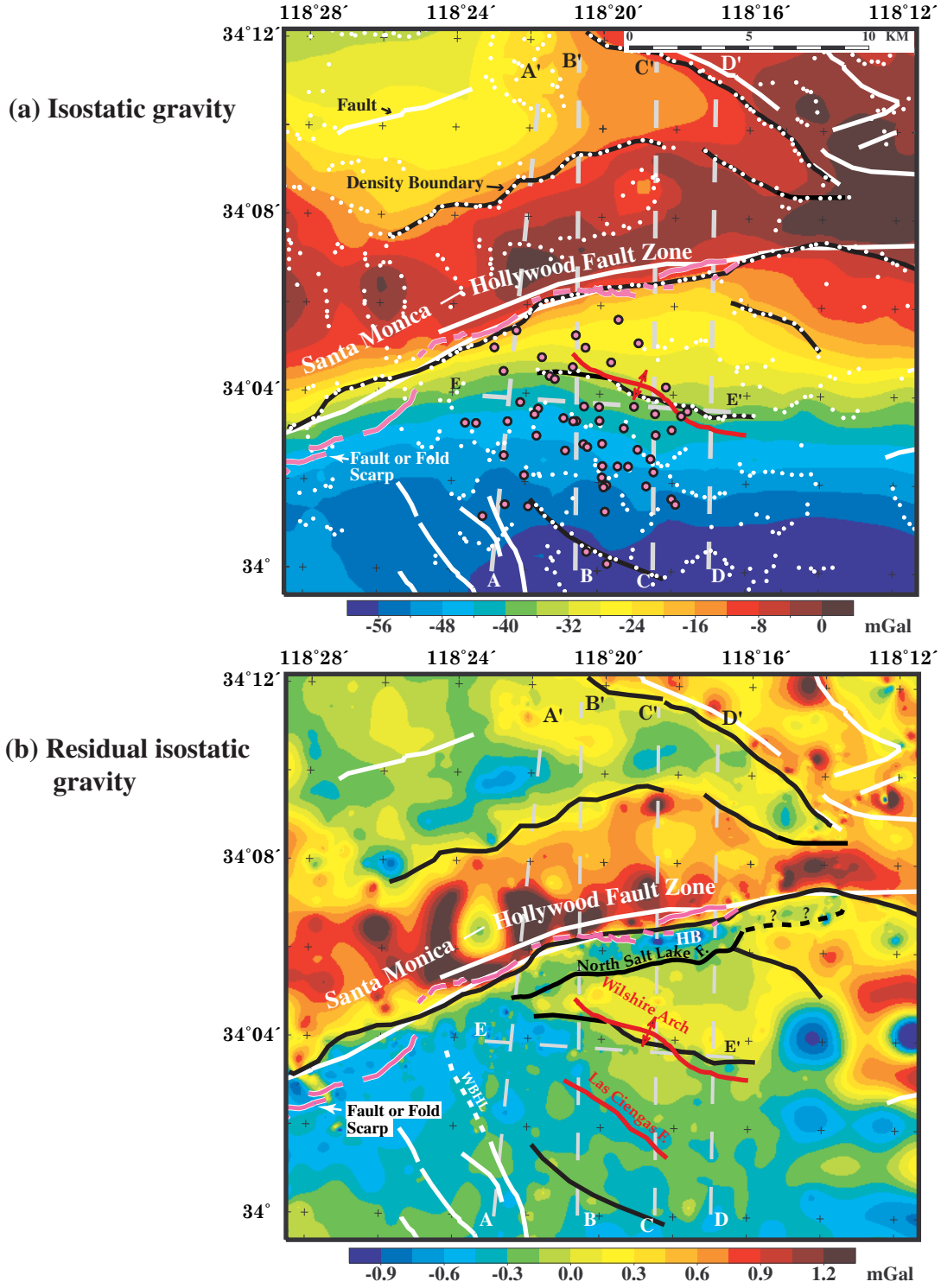

Figure 5. (a) Isostatic gravity map of the northern Los Angeles region. Black lines are interpreted density boundaries based on maximum horizontal gradient magnitudes marked by small white dots. Magenta circles show locations of wells used by Hummon (1994) to construct cross sections. (b) Residual gravity map created by subtracting an upward continued (0.1 km) gravity field from the unfiltered isostatic field (a). Dashed black line defines the interpreted southern boundary of the Hollywood basin (HB). Inversion of the gravity data along profiles AA' – EE' (gray-dashed lines) led to interpretive geologic models (for example, Figs. 7 and 8). Magenta lines are major fault and fold scarps located with boreholes and trenching and by geomorphological mapping by Dolan and others (1997). Red lines highlighting the Wilshire arch and Las Cienegas fault are taken from Hummon (1994). White lines and dashed lines are, respectively, faults from Jennings (1991) and the West Beverly Hills lineament (WBHL).

named GMSYS (names of private products are for descriptive purposes only and do not imply endorsement by the U.S. Geological Survey), which is an interactive, elaborate version of SAKI (Webring, 1985). GMSYS is based on generalized inverse theory. The program requires an initial estimate of model parameters including depth, shape, magnetization, and density of suspected sources, and then varies selected parameters in an attempt to reduce the weighted root-mean-square error between the observed and calculated magnetic and gravity fields.

Interpretive solutions of gravity data using such inverse modeling techniques are nonunique, because an infinite number of geometrical models satisfy the observed field. Available surface geology, drill-hole data, measured lithologic properties, and geologic reasoning substantially reduce the ambiguity and aid in the formation of a reasonable model.

Representative densities

Drill-hole data, density measurements on rock samples, and seismic wave velocity measurements are used to constrain the densities assumed in the models. We also assume that only minor lateral density variations occur within discrete lithologic bodies, so that densities can be inferred where only lithologic data are available. Densities associated with lithologic units and density-depth relations were estimated from gamma-gamma compensated formation density logs and simultaneous compensated neutron-gamma formation density logs from drill holes, some reaching depths of more than 3 km (for example, Figs. 6 a-c).

Density of near surface material (above about 30 m) was estimated using seismic-wave velocity and density relationships, leading to a representative density of 2.02 g/cm^3. More than 50,000 bulk density measurements within the top 400 m, using gamma-ray attenuation from 779 wells in the Los Angeles region, lead to an average density of 2.04 g/cm^3, the selected representative density of the Quaternary rocks used in our models. Although near-surface sediment density is highly variable, roughly ranging from 1.4 and 2.2 g/cm^3 (Fig. 6), we assume that the average density over the entire Quaternary section approaches the calculated average value of 2.04 g/cm^3.

The assumed densities of the remaining Cenozoic section are based partly on drill-hole data and burial depth, such as shown in Figure 6. McCulloh (1967) provided relationships between porosity and depth based on laboratory measurements of more than 4,000 cores, mainly from the Los Angeles Basin and nearby basins. Assuming that the typical sedimentary section in the northern Los Angeles Basin has associated porosities lying between the probable maximum average porosity of reservoir sandstone and the minimum porosity in an argillaceous rock, the resulting average porosity versus depth relationship (using McCulloh's Fig. 4) was used to calculate the densities shown in Figure 6d. Beyond the clear observation that density increases with depth, these results suggest that density changes rapidly at depths less than 1 km, ranges in density from 2.2 to 2.5 g/cm^3 between 1 and 5 km, and approaches 2.6 g/cm^3 at depths greater than 7 km.

The depositional environment of the sedimentary units was also used to select changes in density with depth. For example, a marked deepening of the basin from neritic to upper bathyal depths may result in a shift in formations

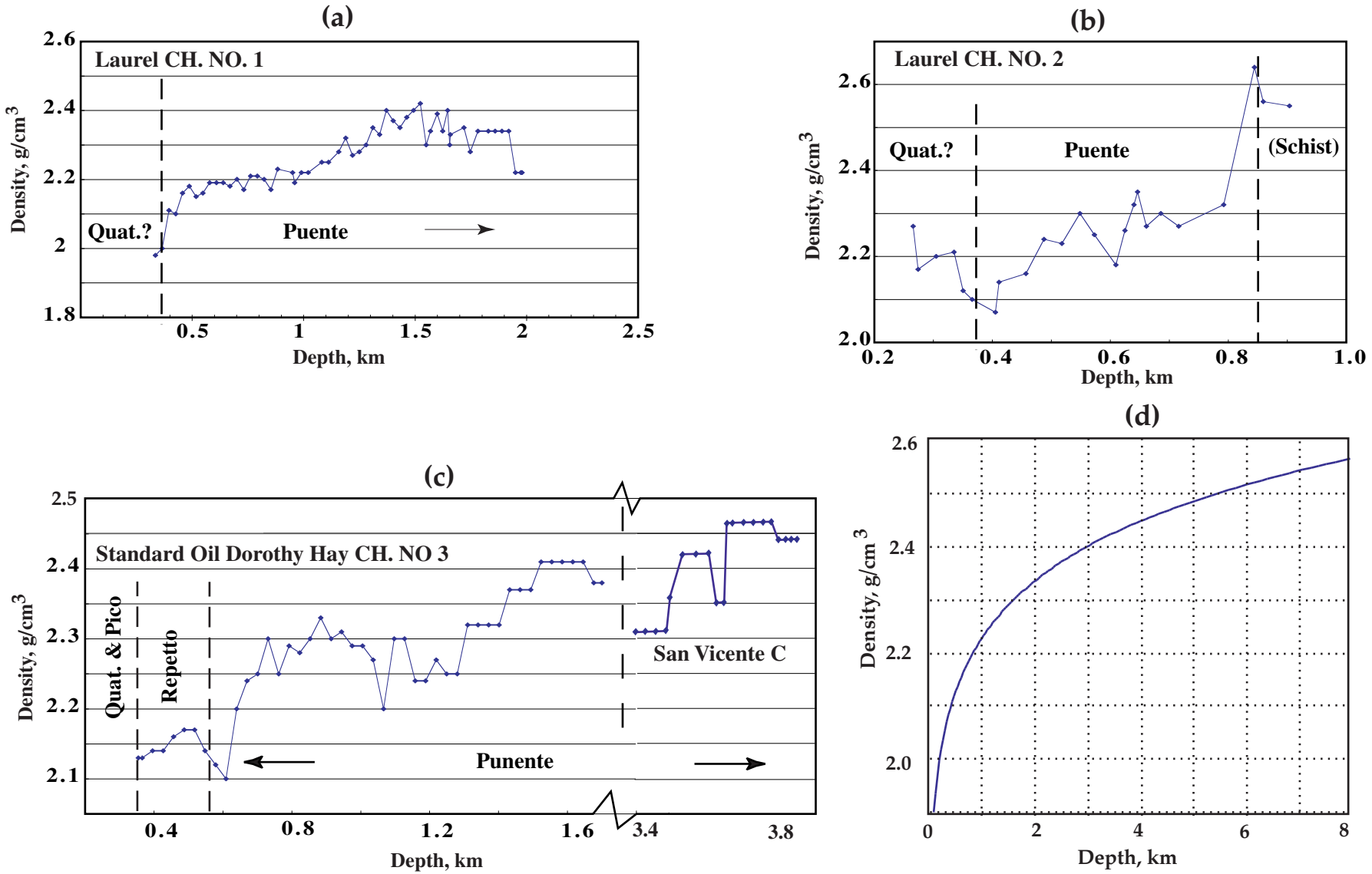

Figure 6. Density versus depth based on gamma-gamma compensated logs in the a. Laurel CH1 (LC1, Fig. 4), b. Laurel CH2 (LC2, Fig. 4), and c. Standard Oil Dorothy Hay CH3 and San Vicente C wells (both at SV, Fig. 4). d. Calculated density versus depth derived from porosity-depth relationships based on laboratory measurements on cores by McCulloh (1967). We assumed the typical sedimentary section in the northern Los Angeles Basin has associated porosities lying between the probable maximum average porosity of reservoir sandstone and the minimum porosity in an argillaceous rock. The plots show density generally increases with depth. At depths of more than 1 km, Cenozoic sedimentary rock density is typically greater than 2.2 g/cm3 and approaches 2.6 g/cm3 at depths greater than 7 km.

from sandstone to less-porous mudstone and thus to a general increase in density. Based on the density-depth relations (Fig. 6) and the depositional environments of the Cenozoic sediment by Blake (1991), we assigned densities to the pre-Quaternary Cenozoic formations (Fig. 2) as follows: Pico (neritic to middle bathyal)—2.2 g/cm^3, Repetto (lower bathyal)—2.3 g/cm^3, Puente (upper to middle bathyal)—2.4 g/cm^3, and Topanga (neritic to upper bathyal)—2.55 g/cm^3.

Basement rocks in the study area include Catalina schist, Santa Monica slate, meta-igneous rocks, and granitic rocks (Sorenson, 1985; Wright, 1991). Average densities of basement rock samples from outcrops and core range from 2.67 g/cm^3 in the northwest part of the Los Angeles Basin (McCulloh, 1957) to 2.71 g/cm^3 in the San Fernando Valley region (Langenheim and others, 2000). Granite and Santa Monica slate (Fig. 3) typically have densities of about 2.67 g/cm^3 (Langenheim and others, 2000), the selected value for basement rocks in our models. It will be shown, however, that to properly match the observed and calculated fields using the above assumed sediment densities, the density of the basement rocks at a shallow depth (probably < 1 km) beneath these mountains must increase to about 2.74 g/cm^3 to generate the prominent gravity highs over the Santa Monica Mountains.

Inversion approach

Four north-south profiles normal to the gradients of the major gravity features (Profiles AA'-DD', Figs. 5a) were selected at representative locations along the length of the Hollywood basin to cross regions of greatest gravity station density and good well data concentration. A fifth, east-west profile (EE') was modeled (results not shown here) to tie the results of AA'-DD' together (in other words, to ensure that the north-south models agree with each other). Profile AA' was selected because of the significant drill-hole information along it, but gravity coverage is poor (Fig. 4). Therefore, unlike the other profiles where the observed field is based on gravity stations projected onto the profile (Fig. 7 b-d), the observed gravity field for Profile AA' (Fig. 7a) was taken from the grid shown in Figure 5a. Station locations along Profiles BB'-DD' are generally spaced 200 m apart near major gravity features. Distant from the areas of interest, profile data resolution is about one station every kilometer, except along profile C where a 2 km gap over the Santa Monica Mountains exists. Although the profiles extend northward across the Santa Monica Mountains into the San Fernando Basin, we show here only the model results over the southern and middle parts of profiles to examine the Hollywood Fault and basin. Long profiles and deep well data are necessary to properly model the regional anomalies. A realistic model that adequately explains the observed regional anomalies leads to a better definition of sources of superimposed, local anomalies, such as the expression of the Hollywood basin.

Along our profiles, many drill holes used by Hummon (1994) to construct geologic cross sections were used to constrain our models. Well depths to the top of the geologic formations shown in Figure 2 were used as control points in the forward modeling process. For example, logs from the Laurel-2 (Profile AA', Fig. 7a) contain lithology and biostratigraphy data that clearly define the top of the Puente formation (340 m) and the metamorphic sedimentary basement rocks (schist) (844 m; Hummon, 1994).

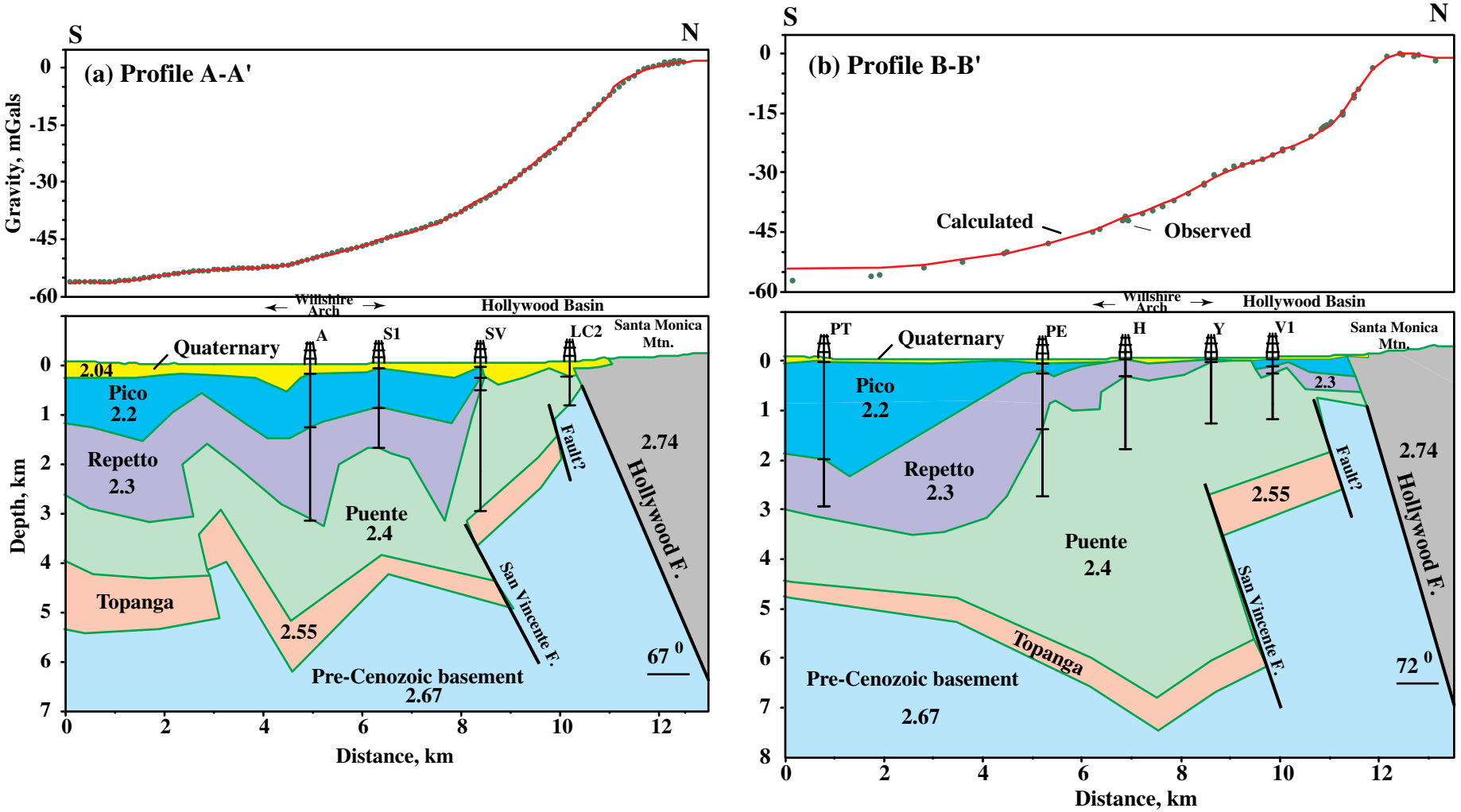

Figure 7. Inversion of gravity data (Fig. 5a) across the Hollywood Fault and basin showing computed and actual gravity fields (upper diagrams) and interpretive model (lower diagrams) for profiles AA' – DD', located in Figures 4 and 5. Numbers are assumed formation densities (g/cm3), also shown in Figure 2. South of the Hollywood Fault, most faults from Hummon (1994) have little gravity expression, largely because the major offsets of density boundaries lie at appreciable depths. Based primarily on the well data and the cross sections compiled by Hummon, we include these faults in our models for completeness. Well labels are defined in Figure 4 caption.

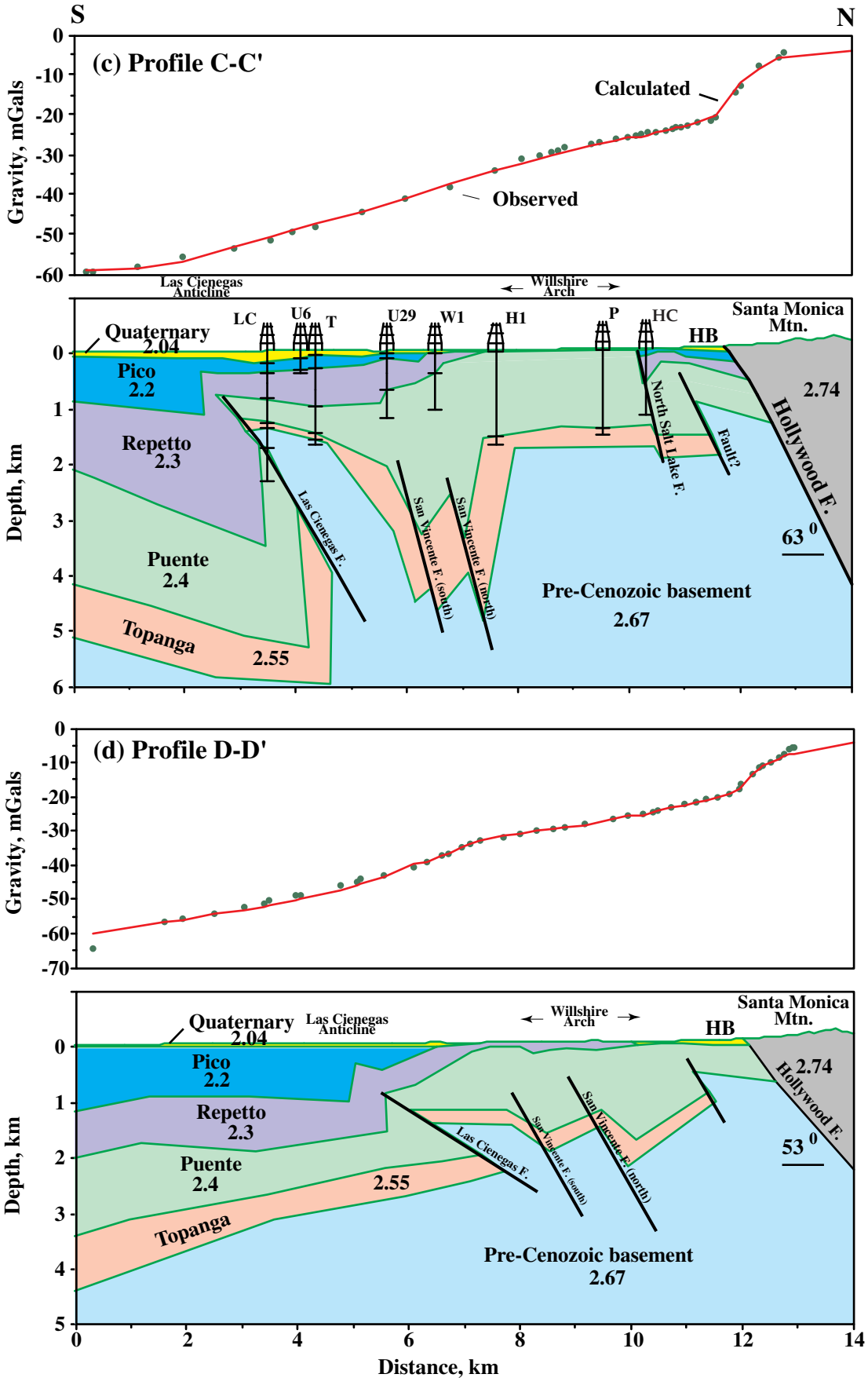
S
N
(c) Profile C-C'
Gravity, mGals
Calculated
Observed
Las Cienegas Anticline
Willshire Arch
LC
U6
T
U29
W1
H1
P
HC
HB
Santa Monica Mtn.
Quaternary 2.04
Pico 2.2
Repetto 2.3
Puente 2.4
Topanga
2.55
Las Cienegas F.
San Vincente F. (south)
San Vincente F. (north)
North Salt Lake F.
Fault?
Hollywood F.
2.74
63 0
Pre-Cenozoic basement
2.67
Depth, km
(d) Profile D-D'
Gravity, mGals
Quaternary 2.04
Las Cienegas Anticline
Willshire Arch
HB
Santa Monica Mtn.
Pico 2.2
Repetto 2.3
Puente 2.4
2.55
Topanga
Las Cienegas F.
San Vincente F. (south)
San Vincente F. (north)
Hollywood F.
2.74
53 0
Pre-Cenozoic basement
2.67
Depth, km
Distance, km

Profile AA': The westernmost profile crosses the city of West Hollywood and continues into Beverly Hills. This profile was chosen primarily because it crosses four petroleum wells providing considerable modeling constraints in the Los Angeles Basin. The steep boundary separating the outcropping, dense plutonic basement (Fig. 2) and the low-density basin fill defines the Hollywood Fault. In out model, the Hollywood Fault dips 67°, but a suitable match between the observed and calculate anomalies is achievable by varying the dip of the Hollywood Fault by 8° (in other words, a dip of 67° ± 8°).

Due to relatively poor gravity coverage along this profile, boundaries for the Hollywood basin are controlled primarily from surface geology and well data. The width of the Hollywood basin is about 2.2 km. Based on the assumed stratigraphy in the Laurel CH-2 well, Hummon (1994) inferred that Quaternary alluvium and marine sand and gravel lie directly above Miocene (middle Puente) strata (Figs. 2, 4, and 6). Assuming the fill consists only of Quaternary sediments (2.04 g/cm^3), an average depth to the Puente formation is about 300 m (Fig. 7a), which is consistent with the well data.

In the Los Angeles Basin, sharp undulations in the basement surface generally reflect the presence of vertical movement along faults. South of the Hollywood Fault, most faults from Hummon (1994) along Profile AA' have little gravity expression, largely because the major offsets of density boundaries lie at appreciable depths and thus their effects are small. Based primarily on the well data and the cross sections compiled by Hummon, we include these faults in our models for completeness.

Profile BB': Profile BB' (Fig. 7b) follows La Brea Avenue in Hollywood and also has good well control (5 wells) for the low-density sedimentary formations. Gravity stations are dense along this profile, particularly in the central and northern parts of the Los Angeles Basin. The Puente formation overlies large basement offsets, possibly related to thrust faults (Hummon, 1994). The Hollywood Fault dips to the north at about 72° (± 8°) in our model. The gravity data, which are particularly useful in defining the location of the Hollywood Fault (normally assumed to be at the northern margin of the Hollywood basin) suggest that the fault extends (~ 400 m) into the basin south of the exposed juxtaposition of granite and Quaternary sediments (Fig. 8). Our results indicate that the Hollywood basin is about 2 km wide along Profile BB'.

To understand the range of reasonable thickness of the Hollywood basin fill, we explore alternative density models (and thus stratigraphic units) above the Puente formation. The reason to vary the basin fill stems from the conflicting well data. In the Laurel CH-2 well (Fig. 7a), Quaternary sediment may lie directly above Puente sediment (Hummon, 1994). On the other hand, in the Standard Vista and Texas Hollywood CH1 wells (Figs. 7b,c and 8), Quaternary alluvium and Pliocene siltstone and shale are identified above the Puente formation (Hummon, 1994). Figure 8 highlights the two basin-fill models for profile B-B', which the gravity inversion process is unable to differentiate. The depth of the Hollywood basin is between about 200 m assuming only a Quaternary sedimentary fill (Fig. 8a) and 600 m assuming the presence of Pico and Repetto as well (Figs. 7b and 8b). For the previous profile AA', if the more dense Pico (2.2 g/cm^3) and Repetto (2.3 g/cm^3) underlie a much thinner Quaternary layer the basin thickness increases from 300m to about 600 m.

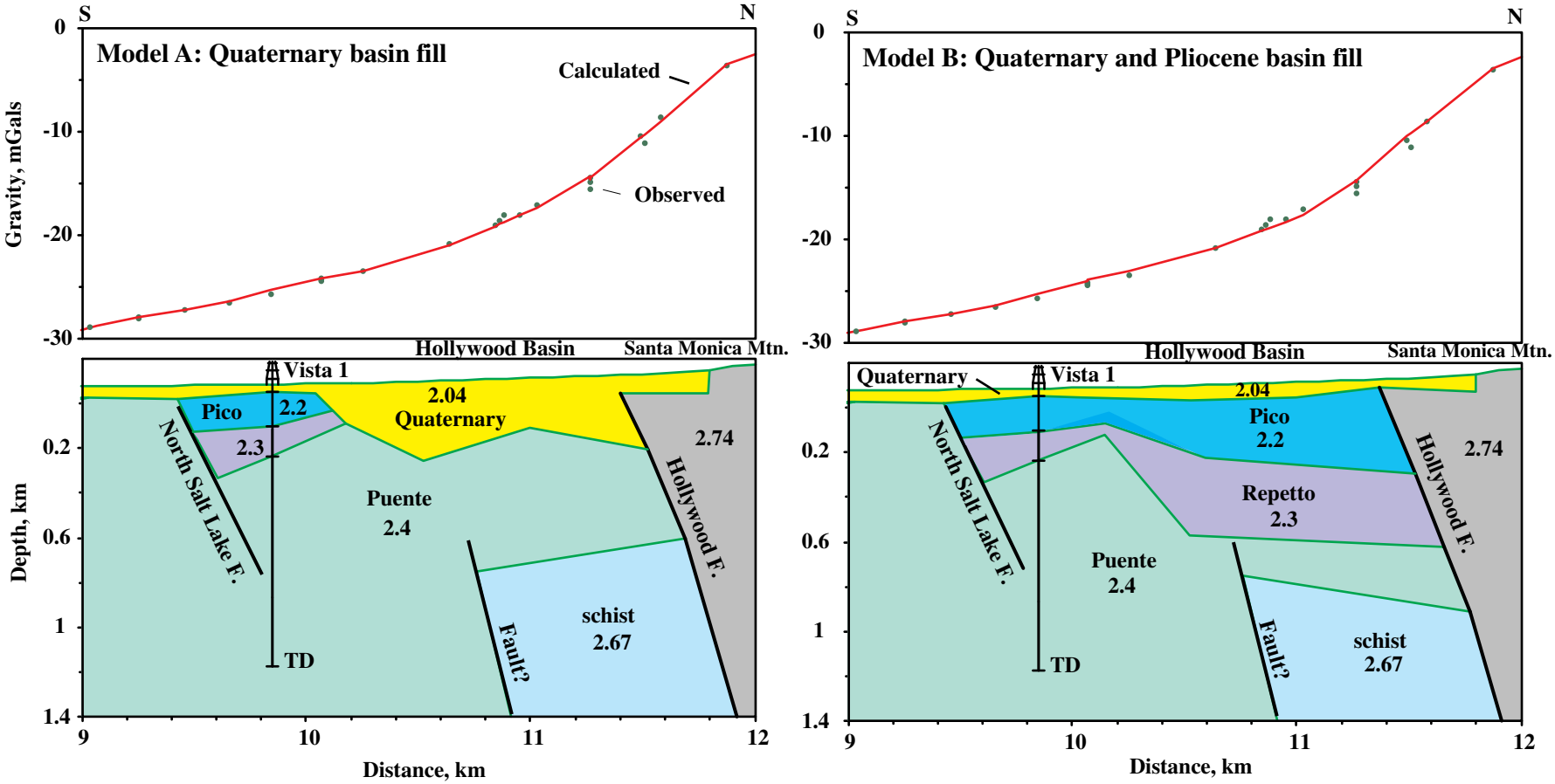

Figure 8. Two undistinguishable density models of the Hollywood basin based on different basin fill along profile BB' (Fig. 7b). Model A is consistent with Laurel CH2 well data (LC2, Figs. 4 and 7a), which suggest Quaternary fill above Miocene rocks. Alternatively, model B is consistent with the Standard Vista CH1 well data (V1, Figs. 4 and 7b) and the Texaco Hollywood CH1 well data (HC, Figs. 4 and 7c), which suggest that Quaternary deposits overlie Pliocene rocks. In this alternative model, the average basin depth (~ 600 m) is over 2 times as great as that in model A (~200 m) to compensate for denser basin fill.

The models (Figs. 7a, 7b, and 8) include an inferred fault near the axis of the deepest part of the Hollywood basin, based largely on the need to include dense schist beneath the basin (Laurel CH-2, Fig. 7a) and the need to abruptly terminate the schist to match the observed and calculated gravity fields.

Profile CC': Profile CC' lies along Western Ave and also has good well control (8 wells) for the low-density sedimentary formations in the Los Angeles Basin. The density of gravity stations is high over the Hollywood basin but thins outside the basin with a large gap over the Santa Monica Mountains. For the present study of the Hollywood Fault and basin, this large gap does not pose a problem since the existing gravity data between the Los Angeles Basin and the Santa Monica Mountains constrain the associated gravity gradient. The Hollywood Fault dips 63° (± 5°) and, unlike in Profiles AA' and BB', appears not to extend south beneath the Quaternary and into the Hollywood basin. Depth to the Puente formation assuming a Quaternary fill (2.04 g/cm^3) in the Hollywood basin leads to a depth of about 200 m (not shown), but modeling the basin with Pico (2.2 g/cm^3) and Repetto (2.3 g/cm^3) underlying the Quaternary alluvium yields a Puente depth of about 500 m (shown in Fig7c).

Profile DD': Profile DD' follows Hoover Ave. Compared to the other profiles, gravity station density is the highest but well control is the least. The model suggests that the Hollywood Fault dips 53° (± 9°). The Hollywood basin is roughly 120 m thick for Quaternary fill (shown in Fig. 7d) or 250 m thick with additional Pico and Repetto fill (not shown).

DISCUSSION AND CONCLUSIONS

The present gravity study leads to new insights and confirms previous interpretations of geologic structures in the northern part of the Los Angeles Basin region. The prominent gravity gradient (Fig. 5b) expressing the boundary between the dense basement rock in the Santa Monica Mountains and the low-density fill of the Los Angeles Basin clearly defines the main reverse faults of the Santa Monica-Hollywood-Raymond fault zone. The gravity-defined Santa Monica-Hollywood-Raymond fault zone generally follows the active fault and fold scarps located with boreholes and trenching and by geomorphological mapping by Dolan and others (1997). An exception occurs west of longitude 118° 26 (Fig. 5b), where the active fault and fold scarps of Dolan and others lie substantially south of the interpreted maximum displacements along the Santa Monica-Hollywood fault zone. Because the gravity field (Fig. 5) does not indicate a shallow, dense basement in the immediate vicinity of the active strands here, the associated offsets are likely small and young compared to those along the Santa Monica-Hollywood fault zone lying north of the active strands. On the other hand, active strands sometimes lie north of interpreted major basement offsets related to the Hollywood Fault in several places east of 118° 22'. In these regions, the present seismic activity is likely associated with secondary strands of the Hollywood fault zone. Our models (Fig. 7) suggest that the Hollywood Fault dips to the north roughly 63° (calculated values of 53°, 63°, 67°, and 72°).

Other interpreted density boundaries correlate with known geology. For example, the northwest-trending boundary in the northeastern part of the study area (Fig. 5) follows the margin of dense Precambrian rocks (Verdugo Fault,

Langenheim and others, 2000). In the Los Angeles Basin, the Wilshire arch appears as a subtle gravity high south of the North Salt Lake fault (Fig. 5b), possibly expressed as a subtle gravity gradient (Fig. 5b).

Hollywood Basin

Geometry

Hummon and others (1994) provide the most recent description of the Hollywood basin in the form of structural contours on the base of Quaternary strata, using drill hole data and interpretive geologic cross sections. The limited amount of subsurface information forced Hummon and others (1994) to speculate about the eastern extent of the basin (dashed magenta contours, Fig. 9). The gravity field with enhanced expressions of shallow sources (Fig. 5b) suggests that the basin flanks the range front faults on the south from, at least, longitude 118° 23′ to 118° 16′ (> 12 km). One might extend the basin eastward to 118° 14′ (Fig. 5b). Tsutsumi and others (2001) proposed that the western terminus of the basin lies at the West Beverly Hills lineament (118° 27′; Fig. 1), although there is no well control to support this extension. No subtle gravity expression of the basin is apparent west of 118° 23′, but it could be masked by more intense lows related to a thicker sedimentary section in the adjacent Los Angeles Basin to the south.

The range front thrust generally represents the northern margin of the Hollywood basin, but it underlies the basin between longitude 118° 20′ and 118° 22′ (about 400 m south of active fault and fold scarps; Figs. 8 and 9). The location of the southern margin of the basin hinges on the associated structural model as discussed below. If the North Salt Lake fault is assumed to be the southern margin, the Hollywood basin is defined as a narrow trough (approximate maximum width – 2 km; approximate maximum average depth – 600 m). The gravity gradient related to the North Salt Lake fault is not steep (Fig. 5b), due to one or more of the following: (1) fault dip is considerably shallower than presently assumed from drill hole data, (2) the lateral density variation across the fault is minimal, and (3) the predicted but unobserved gravity low north of the fault is offset by shallow, relatively dense Puente north of the fault (as shown in Fig. 8).

The modeled basin floor undulates, perhaps reflecting vertical offsets along a fault(s) (Fig. 8). Our gravity models, constrained by Laurel CH-2 well, include a fault near the axis of the Hollywood basin, based largely on the need for dense schist (based on well data) and the need to abruptly terminate it beneath the basin. The inferred axial fault may be a strand of the Santa Monica–Hollywood fault zone or a local fault analogous to the North Salt Lake fault.

Origin

Based on our gravity models, we propose that the Hollywood basin is a flexural basin or basement monocline formed by thrust faults along the Santa Monica-Hollywood fault zone. Thus the Hollywood basin is analogous to foreland basins formed due to lithospheric flexure in response to similar overthrust loading. In our models (see Figs. 7 and 8), a thickening of basin fill northward to the Hollywood Fault is required to match the steep gravity gradient and is consistent with a basin origin related to flexure. What is the role of the North Salt Lake fault, because the proposed monocline formed by flexural loading would have no faulted southern margin? We suggest that the North Salt

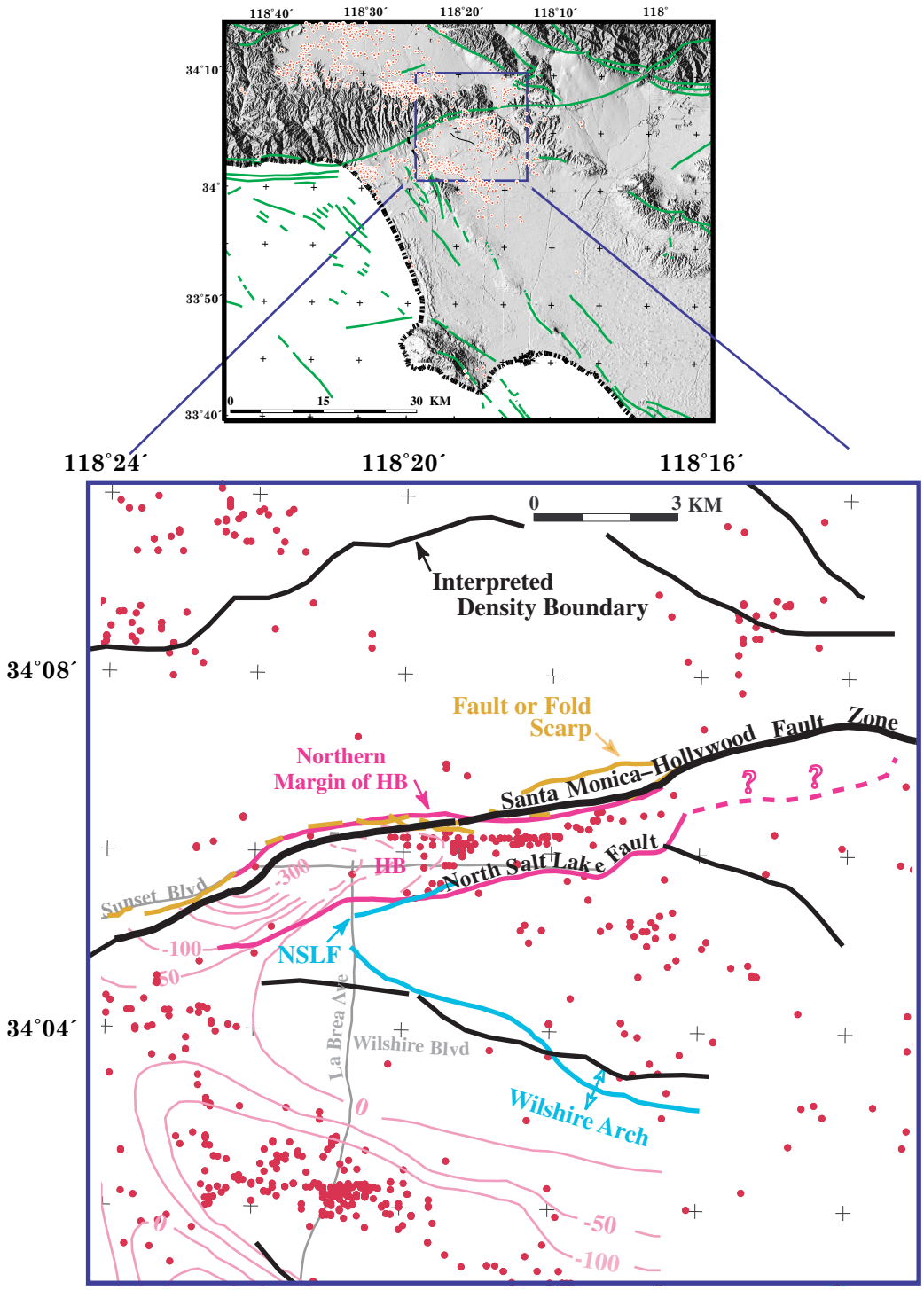

Figure 9. Interpreted structures and locations of structures damaged by 1994 Northridge earthquake. The pattern of red tagged structures (red dots) displays a strong spatial correlation with the axis of the interpreted Hollywood basin (HB). Black lines are interpreted density boundaries. The northern margin of the Hollywood basin and the North Salt Lake fault (magenta lines) are based on the interpretation of the gravity data. The southern basin margin is the inferred location of the North Salt Lake fault. The northern margin of the Hollywood basin often deviates from the interpreted range front fault zone. Magenta structural contours on the base of Quaternary (50 m interval) from drill hole data and interpretive geologic cross sections is taken from Hummon and others (1994). Orange lines are fault and fold scarps located with boreholes and trenching and by geomorphological mapping by Dolan and others (1997). Cyan lines highlighting the Wilshire arch and North Salt Lake fault are taken from Hummon (1994). Green lines on shaded relief map are faults taken from Jennings (1994).

Lake fault either formed or was reactivated during flexural loading as a normal fault, resulting in the narrow Hollywood trough along the range front. Moreover, because of the limited well control and inadequate resolution of the gravity data, we cannot rule out flexural deformation causing a northward thickening of some sedimentary layers from the Wilshire arch (south of North Salt Lake fault) to the Hollywood Fault.

Two other structural models may also be involved in the formation of the Hollywood basin. In the first, Hummon and others (1994) suggested that the Hollywood basin formed between the back limb of a fold above a blind, north-dipping Wilshire fault (see location of Wilshire arch, Fig. 9) and the Hollywood Fault. There is no direct evidence for such a blind thrust fault. Because many other investigators (for example, Shaw and Shearer, 1999; Tsutsumi and others, 2001), however, propose the existence of blind thrusts south of the Hollywood-Raymond fault zone, we cannot rule out a relationship between the Hollywood basin and a back limb of a blind thrust. Like the flexural basin model, the southern flank of the Hollywood basin in the Hummon model would dip gently northward from the Wilshire arch.

The second model, proposed Tsutsumi and others (2001), suggests that the Hollywood basin is a pull-apart structure formed by left slip across the Santa Monica–Hollywood fault zone and right slip along the West Beverly Hills lineament (WBHL, Fig. 1). The existence of a graben is suggested in drill hole data (Standard Vista CH1, Fig. 8), where deeper Repetto layers dip south toward the North Salt Lake fault beneath a relatively flat-lying Pico-Repetto interface. In the graben model, the North Salt Lake fault represents the southern margin of the Hollywood basin. This model leads to a narrow geometry of the basin.

Due to the uncertainty of the basin fill and of the age of reverse and strike slip movement along the Santa Monica–Hollywood fault zone, we are unable to suggest the optimal structural model for the origin of the Hollywood basin. Although our modeling results are consistent with a basin origin related to flexure, we cannot discount contributions to the basin thickening related to a pull-apart graben and a back limb of a blind thrust.

If we adopt the initiation of thrusting at 7 Ma as proposed by Wright (1991) and the time of strike slip movement (7–3.7 Ma) proposed by McCulloh and others (2001), the basin fill should include Repetto, Pico, and Quaternary sediments. Thus, our modeled average thickness of the Hollywood basin that includes Pliocene fill (Fig. 8b) likely applies and ranges roughly from 250 m along profile DD' to 600 m along profile BB'. Due to the uncertainty in the relation between density and depth in the Hollywood basin, these thicknesses should be viewed as poorly constrained with possible errors up to several hundreds of meters. One source of model error, for example, may be related to the assumed representative density of the Quaternary sediment (2.04 g/cm^3), because the bulk density of individual Quaternary layers can vary widely (~ 1.4 to 2.2 g/cm^3; Fig. 6).

To gain additional insights on the Hollywood basin fill, axial fault, and margins, we recommend drilling, additional density measurements, and shallow seismic experiments to better constrain future modeling efforts. The interpretive results shown in Figures 5b, 7, 8, and 9 might be useful in siting where additional data would be useful.

Earthquake Hazard Implications

The Federal Emergency Management Agency (FEMA) conducted an assessment of building damage immediately after the Northridge earthquake in 1994 (M_w 6.7). Locations of buildings classified as unsafe for occupancy were "red tagged" (FEMA, 1994). The pattern of red-tagged structures (Fig. 9) includes a linear concentration of damage that extends along the axis of the gravity-defined Hollywood basin for most of its length. East of 118° 18′, both the trend of red-tagged buildings and orientation of the basin axis change to a more northeasterly orientation.

Clusters of damage distant from the source area, such as observed here, are likely due to multiple factors. Stewart and others (1994) concluded that the distribution of damage in Hollywood shows a clear correlation with the presence of young, soft, near-surface sediments, suggesting that these sediments played a key role in amplifying ground motions. It is well known that soft sediments can amplify ground motion. Hartzell and others (1997) and others proposed that although investigators usually relate site amplification and physical properties, deeper geologic structures (in the upper 1-2 km) can have a significant or even controlling impact on the ground motions at a given site. The tight alignment of damaged buildings along the axis of the Hollywood basin suggests that deeper basin structures affected ground motion related to the Northridge earthquake. For example, the localized damage may be related to the inferred axial fault beneath the Hollywood basin (Figs. 7 and 8), which may have focussed the seismic energy in some fashion.

Significant basin induced effects may lead to strong ground motions. Graves (1995) suggested that in the northwest portions of the Los Angeles region, the observed site responses can be explained with both large and small scale geologic structures (for example, the deep Los Angeles Basin and its sub-basins, respectively). He proposed that body waves generate surface waves by interacting with the margin of the Los Angeles Basin. Kawase (1996) demonstrated that basin edge effects, caused by the constructive interference of direct s-waves with basin-induced diffracted waves, led to a damage belt in Kobe, Japan. Resonance, focussing, and directional effects may also play an important role in determining site response (Hartzell and other, 1997). Focusing and directional effects can be caused by differential refraction of seismic rays that pass through non-planar velocity structures (for example, basin floor or a local anticline on the basin floor), analogous to the focusing of visible light by glass lenses (Joyner and others, 1981; Hartzell and others, 1997). In short, many geological factors may have led to extreme total ground motion amplification in the Hollywood area following the Northridge earthquake.

Because of the localized damage toward the center of the Hollywood basin, our preferred site response factors involve both focussing of energy along an inferred axial basin fault and focussing and directional effects, perhaps related to topography on underlying layers. The presence of young, soft, near-surface sediments is likely an additional factor for the amplified ground motion.

Future research directions to gain more insights on the earthquake hazard in the Hollywood area might include (1) generation of site response models using the geometry of the Hollywood basin determined in the present study, (2) examination of the records of nearby Northridge aftershock stations equipped with velocity transducers and accelerometers to better understand the linear

pattern of red-tagged structures, (3) a study of well data to map variations in sediment physical properties across the Hollywood basin, (4) deployment of additional sensors near the basin axis to measure the site response of future earthquakes, and (5) a more detailed study of the relationship of the gravity-defined range front faults and active strands of the Santa Monica-Hollywood fault zone.

ACKNOWLEDGEMENTS

This study has greatly benefited from reviews by Carl Wentworth and Bob Jachens. Ed Cranswick and Steve Hartzell kindly provided very useful information regarding causes for the amplification of ground motion related to earthquakes.

REFERENCES

Blake, G. H., 1991, Review of the Neogene biostratigraphy and stratigraphy of the Los Angeles Basin and implication for basin evolution, *in* Biddle, K. T., ed., Active margin basins: American Association of Petroleum Geologists Memoir 52, p. 135-184.

Blakely, R.J., and Simpson, R.W., 1986, Locating edges of source bodies from magnetic and gravity anomalies: Geophysics, 51, p. 1494-1496.

Campbell, R. H., and Yerkes, R.F., 1976, Cenozoic evolution of the Los Angeles basin area-relation to plate tectonics, *in* D. G. Howell, ed., Aspects of the geologic history of the California continental borderland: Pacific Section, AAPG Miscellaneous Publication 24, p. 541-560.

Cordell, L., Keller, G.R., and Hildenbrand, T.G., 1982, Bouguer gravity map of the Rio Grande rift, Colorado, New Mexico, and Texas: U.S. Geological Survey Geophysical Investigations Map, GP-949, scale 1:1,000,000.

Davidson, J. G., Berg, M. J., Hamilton, J. C., 1999, Principal facts for 300 gravity stations in the vicinity of Los Angeles and Hollywood, California: U.S. Geological Survey Open-File Report 99-577, 14 p.

Dibblee, T. W., Jr., 1982, Geology of the Santa Monica Mountains and Simi Hills, southern California, *in* D. L. Fife and J. A. Minch, eds., Geology and mineral wealth of the California Transverse Ranges: Santa Ana, California, South Coast Geological Society, p. 94-130.

Dolan, J.F., Sieh, K., Rockwell, T.K., Guptill, P., and Miller, G., 1997, Active tectonics, paleoseismology, and seismic hazards of the Hollywood fault, northern Los Angeles basin, California: Geological Society of America Bulletin, v. 109, p. 1596-1616.

Dolan, J.F., Stevens, D., and Rockwell, T.K., 2000, Paleoseismologic evidence for an early to mid-Holocene age of the most recent surface ruptures on the Hollywood Fault, Los Angeles, California: Seismological Society of America Bulletin, v. 90, p. 334-344.

Durrell, C., 1954, Geology of the Santa Monica Mountains, Los Angeles and Ventura counties, *in* R. H. Jahns, ed., Geology of southern California: California Division of Mines Bulletin 170, map sheet 8.

Eckis, R., 1934, South coastal basin investigations—Geology and ground water storage capacity of the valley fill: California Division of Water Resources Bulletin 45, 279 p.
Federal Emergency Management Agency (FEMA), 1994, Building and Safety Structure Damage Assessment, Northridge Earthquake Disaster, DR-1008, map.
Graves, R.W., 1995, Preliminary analysis of long-period basin response in the Los Angeles region from the 1994 Northridge earthquake: Geophysical Research Letters, v.22, .2, p. 101-104.
Hartzell, S., Cranswick, E., Frankel, A., Carver, D., and Meremonte, M.,1997, Variability of site response in the Los Angeles urban area: Seismological Society of America Bulletin, 87, p. 1377-1400.
Hummon, C., 1994, Subsurface Quaternary and Pliocene structures of the Northern Los Angeles Basin, California [M.S. Thesis]: Corvallis, Department of Geosciences Oregon State University, 109 p.
Hummon, C., Schneider, C.L., Yeats, R.S., Dolan, F., Sieh, K.E., and Huftile, G.J., 1994, Wilshire fault—Earthquakes in Hollywood?: Geology, 22, p.291-294.
Jachens, R.C., and Roberts, C.W., 1981, Documentation of a FORTRAN program, 'isocomp', for computing isostatic residual gravity: U.S. Geological Survey Open-File Report 81-574, 26 p.
Jennings, 1994, C.W., 1994, Fault activity map of California and adjacent areas: California Division of Mines and Geology, California Geologic Data Map 6, scale 1:750,000.
Kawase, H., 1996, The cause of the damage belt in Kobe: The basin-edge effect, constructive interference of the direct s-wave with the basin-induced diffracted/rayleigh waves: Seismological Research Letters, 67, p. 25-34.
Lamar, D. L., 1961, Structural evolution of the northern margin of the Los Angeles basin [Ph.D. dissertation]: Los Angeles, California, University of California, Los Angeles.
Langenheim, V. E., 1999, Gravity data collected along the Los Angeles regional seismic experiment (LARSE) and preliminary model of regional density variations in basement rocks: U.S. Geological Survey Open-File Report 99-388, 22 p.
Langenheim, V.E., Griscom, A., Jachens, R.C., and Hildenbrand, T.G., 2000, Preliminary potential-field constraints on the geometry of the San Fernando basin, Southern California: U.S. Geological Survey Open-File Report 00-219, 34 p.
Luyendyk, B. P., Kamerling, M.J., and Terres, R., 1980, Geometric model for Neogene crustal rotations in southern California: GSA Bulletin, v. 91, p. 211-217.
McCulloh, 1957, Simple Bouguer gravity and generalized geologic map of the northwestern part of the Los Angeles basin, California: U.S. Survey Geological Survey Geophysical Investigations Map GP-149.
McCulloh, T.H., 1967, Mass properties of sedimentary rocks and gravimetric effects of petroleum and natural-gas reservoirs: U. S. Geological Survey Professional Paper, Report: P 0528-A, p. A1-A50.
McCulloh, T.H., Beyer, L.A., and Morin, R.W., 2001, Mountain Meadows Dacite—Oligocene intrusive complex that welds together the Los Angeles

basin, northwestern Peninsular Ranges and central Transverse Ranges, California: U.S. Geological Survey Professional Paper 1649, 32p.
Morelli, Carlo, Gantar, C., Honasala, Taunao, McConnel, R.K., Tanner, J.G., Szabo, Bela, Uotila, U.A., and Whalen, G.T., 1974, The International Gravity Standardization Gravity Net 1971 (I.G.S.N. 71): Paris Bureau Centrale de l'Association Internationale de Geodesie Special Publication 4, 193p.
Shaw, J.H., Shearer, P.M., 1999, An elusive blind-thrust fault beneath metropolitan Los Angeles: Science, v. 282, p. 1516-1518.
Sorensen, S.S., 1985, Petrologic evidence for Jurassic , island-arc-like basement rocks in the southwestern Transverse Ranges and California continental borderland: Geological Society of America Bulletin, v. 96, p. 997-1006.
Stewart, S., Bray, J.D., Seed, R.B., and Sitar, N., 1994, Preliminary report on the principal geotechnical aspects of the January 17, 1994 Northridge earthquake: Earthquake Engineering Research Center Report No. UCB/EERC 94-08, University of California, Berkeley, p. 245.
Tsutsumi, H., Yeats, R.S., and Huftile, G.J., 2001, Late Cenozoic tectonics of the northern Los Angeles fault system: California: Geological Society of America Bulletin, v. 113, n. 4, p. 454-468.
Webring, M., 1982, MINC-A Fortran gridding program based on minimum curvature: U.S. Geological Survey, Open-File Report 81-1224, 43 p.
Webring, M., 1995, SAKI-Fortran program for generalized linear inversion of gravity and magnetic profiles: U.S. Geological Survey, Open-File Report 85-122, 29p.
Wright, T.L., 1991, Structural geology and tectonic evolution of the Los Angeles basin: AAPG Memoir 52, p. 35-134.
Yerkes, R.F., McCulloh, T.H., Schoellhamer, J.E., and Vedder, J.G., 1965, Geology of the Los Angeles basin, California-an introduction: US Geological Survey Professional Paper 420-A, 57 p.
Yeats, R. S., 1968, Rifting and rafting in the southern California borderland, *in* W.R. Dickinson and A. Grantz, eds., Proceedings of the conference on geologic problems of the San Andreas fault zone: Stanford University Publications, Geological Sciences, v. XIII, p. 307-322.